



ISSN ONLINE: 2447-0228







RESEARCH ARTICLE

OPEN ACCESS

INFLUENCE OF CUTTING PARAMETERS ON SURFACE INTEGRITY AND MACHINING FORCES IN TOP MILLING OF METALLIC SPRAYING METAL COATINGS

Carlos Jorge Leão de Oliveira*¹, Rafael da Cunha Hamano², Tatiane de Campos Chuvas³ and Hector Reynaldo Meneses Costa⁴

^{1,2,3,4} Postgraduate Program in Mechanical Engineering and Materials Technology, Federal Center for Technological Education Celso Suckow da Fonseca – CEFET-RJ, Rio de Janeiro, Brazil.

¹ <http://orcid.org/0000-0002-2554-9775> , ² <http://orcid.org/0000-0002-6811-5328> , ³ <http://orcid.org/0000-0002-7512-4193> ,
⁴ <http://orcid.org/0000-0002-0887-6838> 

Email: *cjleao216430@gmail.com, rafaelhamano@gmail.com, chuvas.tatiane@gmail.com, hectorrey@gmail.com

ARTICLE INFO

Article History

Received: May 24th, 2022

Accepted: June 28th, 2022

Published: June 30th, 2022

Keywords:

Thermal arc spray,
Milling,
Machining forces,
Surface integrity,
Tool wear.

ABSTRACT

This work aims to evaluate the behavior of coatings applied by electric arc thermal spraying on a low carbon steel substrate when subjected to a milling process under different cutting conditions (cutting speed and tool tip radius). It was observed how these cutting conditions influenced the surface integrity of the machined part (roughness) and the machining forces generated during the process. An evaluation of the types and levels of tool wear in the milling operations was carried out. To obtain the results, samples of ASTM-A36 steel sheets thermally sprayed with and without sealant were milled with cutting speeds of 50 m/min and 84 m/min, and inserts with tip radius of 0.4 mm and 0.8 mm. The cutting parameters used were based on previous work and information from the cutting tool manufacturer. The present work identifies that cutting speed set to 50m/min led to lower machining forces and better tool wear performance. The results obtained indicated that the tool with the smallest tip radius provided better cutting conditions, in the coating without application of sealant. The tool with the largest tip radius presented lower machining forces for the application of sealant. There were no expressive differences in the finish of the machined surfaces, but the experimental values obtained for the average roughness (1 μ m to 1,79 μ m) remained in accordance with the limits indicated in the literature. The predominant tool wear was the plastic deformation in the tip of the inserts and crater wear located on rake face.



Copyright ©2022 by authors and Galileo Institute of Technology and Education of the Amazon (ITEGAM). This work is licensed under the Creative Commons Attribution International License (CC BY 4.0).

I. INTRODUCTION

In the search for solutions to increase the useful life of machinery and equipment components, with regard to minimizing (or even inhibiting) the action of agents in environments with aggressive atmospheres, the technological advance in the area of metallurgy with the development of new surface treatment techniques, as described [1].

There are many metallic coating techniques used in the industry. The increase in the number and importance of surface treatment process applications allows replacing traditional applications such as nickel plating, galvanizing, chrome plating,

etc. by thermal spraying [2]. Among the metallization processes, thermal spraying stands out for guaranteeing the protection of the base material without impacting the environment, compared to other coating techniques.

Many thermal spray coatings will certainly undergo machining processes, either to improve surface finish and/or to meet dimensional tolerance requirements for certain projects. Thus, the most accurate decision of machining technology applied to the coating is directly linked to the functionality of the parts for which the coating was defined.

There are several elements present in the structure of sprayed coatings that affect the machining process, such as

partially fused or unfused particles, pores, oxidized particles, and different hard and brittle phases (carbides and oxides). During the machining process, these elements are the cause of intermittent cutting, which leads to rapid wear of the cutting tool, which can affect the desired quality of the thermal coating surface finish that could be achieved. It is also known that other factors that influence the selection of technology and machining parameters concern the set of phenomena that occur because of the cutting process in the surface layers: changes in mechanical properties, structural changes, defects, hardening and residual stresses. However, there are no studies on the behavior of materials sprayed in machining and how the cutting parameters can influence the process [3]. However, machining thermal sprayed coatings is a process for cutting materials that are difficult to machine. In the work performed by [4], the machining by end milling of samples of superalloy Inconel 718 showed, among results, a surface finish ranging from $1.5 \mu\text{m}$ and approximately $2.5 \mu\text{m}$, with cutting speed (V_c) 60 m/min. Comparing this result with the variable surface roughness obtained in milling the coatings sprayed in this work ($1 \mu\text{m}$ to $1.79 \mu\text{m}$), with cutting speed (V_c) 50 m/min, it is possible to observe the existence of proximity in the experimental values found. Thus, similarities in the behavior of these materials are assumed when machining with a tool with defined geometry.

The purpose of this work is to evaluate the influence of cutting parameters (cutting speed and feed per tooth), together with different cutting tool tip radius, on tool wear, machining forces and surface finish by the milling process in metallic coatings based on iron-nickel, iron-chromium, and cobalt-chromium alloys. The coating deposition process was performed by electric arc thermal spraying, which compared to other spraying techniques has advantages such as high deposition rate and lower cost.

II. THEORETICAL REFERENCE

II.1 THERMAL SPRAY

Of the methods of applying metallic coatings, thermal spraying (ts) is a method of great industrial acceptance for bringing together low cost and certain advantages compared to other techniques. This process guarantees a wide range of chemically different materials that can be sprayed, and has a high coating deposition rate, which allows for greater thicknesses of sprayed material, in addition to the portability of the equipment used [5].

The coating structure is formed from the continuous deposition of molten particles that will accumulate a coating characterized by flattened particles and lamellar microstructure [6]. Among the various existing processes, thermal spraying is the one with the most numerous configurations, both in terms of energy sources (plasma, flame, electric arc) and materials used (metals, ceramics, polymers, composites, etc.) [7].

Electric arc thermal spray technology has become popular compared to other spray technologies mainly due to its high thermal efficiency, high spraying efficiency and low processing cost [8].

The coatings produced by thermal spraying have high roughness, which can have undesirable effects on the mechanical set in operation, resulting in greater friction and wear of components, causing changes in the adjustments provided for in the project. To meet these mechanical elements and guarantee them pre-established dimensions, they must be subjected to a precision finishing operation. As a result, coatings are often turned, milled, or ground [9].

II.2 MILLING THERMAL SPRAYED MATERIALS

According to [9], some care must be taken when milling thermally sprayed flat surfaces: priority should be given to removing raised areas or irregularities and making very light cuts; in crosscut tangential milling, care must be taken to avoid lifting the coating from the substrate; cutting speeds should be in the range of 20 to 30 m/min, however, they can be higher when milling some materials, such as copper alloys; the feed is usually $0.2 - 0.5$ mm/revolution for roughing and should be reduced according to the finishing required.

II.3 MACHINING FORCES ANALYSIS

In machining operations where there are interruptions in the cut and variations in the thickness of the cut, as in milling, the analysis of the efforts involved is essential for understanding the mechanical behavior of the tool. According to [10] the main factors that can affect the machining forces are the cutting parameters (mainly the feed), workpiece hardness, shear strength of the machined material, tool geometry and the stability of the machine and the cutting device fixation. In this study, for the simplification and understanding of the machining force analysis, the orthogonal cut hypothesis is adopted. That is, the material to be removed undergoes plane deformation, as it does not deform in the direction of the length of the cutting edge. The deformation of the material occurs on the surface of the tool, in the plane orthogonal to the cutting edge, the work plane [11]. However, it is necessary to understand the theories of orthogonal and oblique cutting for the application in current projects of cutting tools with complex geometries. Because the basic mechanisms for material removal and chip formation remain the same as in classical processes [12].

Having as reference the hypothesis of the orthogonal cut, [11] considers that in the work plane there will be three pairs of components, perpendicular to each other. These pairs will be arranged in three different directions: in the cutting direction, where the cutting force (F_C) is located, forming an orthogonal pair with the advance force (F_F), as shown in figure 1a; towards the tool rake face, placing the friction force (F_T) and perpendicular to the force normal to the rake face (F_N), indicated in figure 1b; in the direction of the shear plane, which contains the shear force (F_Z) followed by the force normal to the shear plane (F_{NZ}), illustrated in Figure 1c.

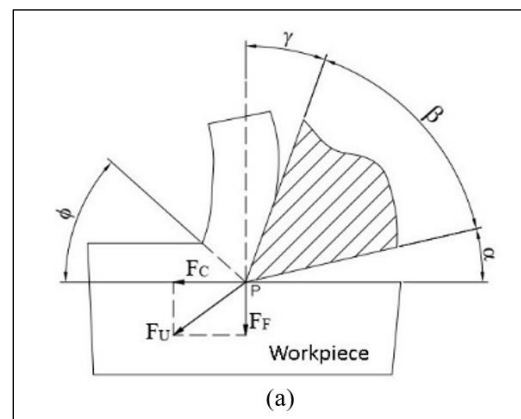


Figure 1a: Machining force components in the work plan: a) cutting force (F_C) and feeding force (F_F).

Source: Adaptation by [11].

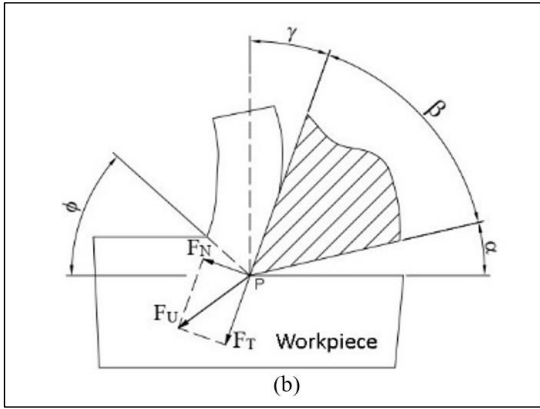


Figure 1b: Machining force components in the work plan: b) frictional force (F_T) and normal force to the output surface (F_N). Source: Adaptation by [11].

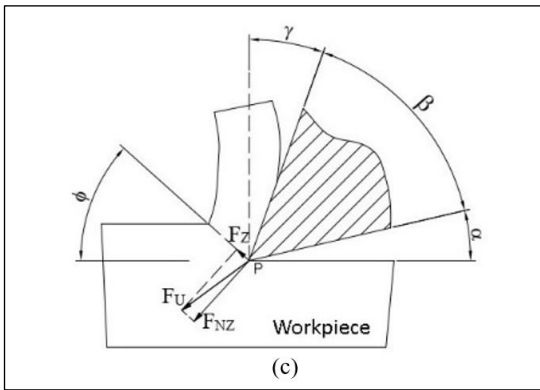


Figure 1c: Machining force components in the work plan: c) shear force (F_z) and normal shear force (F_{Nz}). Source: Adaptation by [11].

II.4 TOOL WEAR EVALUATION

In the cutting tool, the evaluation of the cutting edge is a vitally important factor in defining the tool life in the machine and has a direct influence on the surface quality of the part, its dimensional accuracy and the cost of the final product. In general, wear is mainly influenced by the state of stress and temperature variation in the cutting region and propagates according to several different mechanisms. The presence of Ni favors the increase of resistance to heat and oxidation in materials. Researchers, such as [13], describe that the traditional machining processes of Ni-based materials are challenging, as these alloys usually have low thermal conductivity. For this reason, heat will advance into the tool material, and this causes the tool to wear out.

In the cutting edge, there are three main wears that can occur on cutting tools: flank wear, crater wear, and notch wear.

Flank wear is the most frequent among the wear. It is located on the tool clearance surface and is attributed to the heat generated by friction between the tool flank face and the newly machined surface of the part. For [14], high temperatures on the tool and chip surfaces increase the heat transfer to the tool and accelerate its wear.

Notch wear occurs when machining a hardened (hardened) surface. The notch tends to be a region of stress concentration due to its steep depth, which can lead to rapid and sudden tool failure.

Crater wear occurs on the tool rake surface, where the chip flows, in the secondary shear zone. This wear takes place at high levels of cutting speed and temperature and results from the

combination of abrasion and diffusion wear mechanisms. Crater formation is the result of stress distribution on the tool rake surface.

III. MATERIALS AND METHODS

III.1 SUBSTRATE MATERIAL

For the samples, ASTM A36 carbon steel was used as a substrate and they were made in the form of a ¼" thick plate and chemical composition, according to standard [15], which is shown in Table 1.

Table 1: Chemical composition of carbon steel (% weight).

C	Mn	P _{max}	S _{max}	Si _{max}
0,26	0,85	0,04	0,05	0,40

Source: [15].

III.2 METHODS

III.2.1 Thermal Spraying Process

To obtain the coating, the electric arc thermal spraying process was used. The main characteristics of the process, from blasting to the formation of texturing to the application of the metallic coating, are described in Table 2.

Table 2: Coating process characteristics.

Characteristics	
Process	Thermal spraying
Form of heating	Electrical energy (electric arc)
Application mode	Manual
Sample dimensions	Plate with 100 mm x 150 mm x ¼"
Number of samples	06
Sample preparation	Sandblasting with aluminum abrasive grains
Sample roughness	130 to 150 μm
Application distance	100 mm
Electrode	AISI 420 martensitic stainless steel wire
Electrical characteristics	Voltage: 30 V Amperage: 100 A
Air pressure	7 kgf/cm ²
Coating thickness	1,2 to 1,5 mm
Coating hardness	35 to 400 HRC
Sealant	3 Coats of epoxy resin (on 3 samples)

Source: Authors, (2022).

In the electric arc thermal spraying process, in this research, the wires used (ER420) have a chemical composition, as shown in Table 3.

Table 3: Chemical composition of wires in the thermal spraying process.

C	P	S	Mn	Mo	Cr	Si	Cu	Ni
0,25 to 0,40	0,03	0,03	0,6	0,6	12 to 14	0,5	0,75	0,6

Source: [16].

The samples obtained were divided into two groups: samples sprayed and sprayed with sealant application. In this research, the sealant resin copolymer WFT 1532 was used, which has the characteristic of promoting active capillary sealing of the

porosity of the coating. Figure 2 represents the dimensions and surface characteristics of the samples.

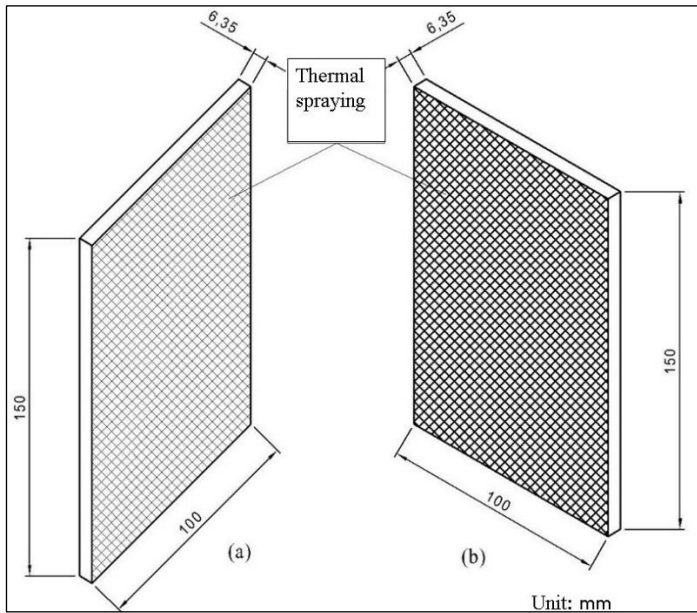


Figure 2: Dimensions and surface characteristics of samples: (a) sample without sealant, (b) sample with sealant
Source: Authors, (2022).

III.2.2 Machining, Machining Forces and Roughness of Samples Thermal Spraying Process

The machining of the samples was carried out in a Diplomat 3001 milling machine, model FVF-2000, at the Machining Research Laboratory (LABUS) at CEFET/RJ. To evaluate the surface treatment applied to the samples and to investigate the mechanical properties of the resulting material, the surface finish (roughness) and the machining force after milling the coating were adopted as evaluation criteria. The milling operation was performed using cutter R390-020 A 20L -11L with Ø20 mm, with two cutting edges and inserts R390-11T3 08M-PM1130 with 0.8 mm of nose radius and R390-11T3 04M-PM1130 with 0, 4 mm nose radius, both from the manufacturer Sandvik. These pellets had AlTiCrN coatings obtained by the physical vapor deposition (PVD) process.

To perform the machining of the samples, channels were milled with a length covering the entire width of the part and a depth of 0.50 mm. The cutting parameters used are shown in Table 4. In all conditions, abundant cutting fluid was used (approximate flow rate of 3.8 l/min). In each condition, a new pair of cutting edges was used, so that the wear did not influence the results obtained.

Table 4: Sample machining conditions.

Parameters	Values
Cutting depth (a_p)	0,50 mm
Cutting speed (V_c)	50m/min and 84m/mmin
Rotation (n)	795RPM and 1337RPM
Forward speed (V_f)	175mm/min and 294mm/min
Feed per tooth (F_z)	0,11mm

Source: Authors, (2022).

In the initial evaluation by machining, a tool with a radius of 0.8 mm was used and the samples were submitted to two levels of cutting speed: 50 m/min and 84 m/min. The initial results,

totalled in four conditions, refer to samples without sealant and with sealant, as shown in Table 5.

Table 5: Sample machining initial conditions.

Condition	Sealant	V_c (m/min)
1	Without	50
2	Without	84
3	With	50
4	With	84

Source: Authors, (2022).

The sprayed metallic coating started to be analyzed through milling, where the influence of the cutting parameters on the useful life of the tools, on the machining forces acting on the cut and on the surface finish resulting from the machining process was evaluated.

For the acquisition of machining force data, a piezoelectric dynamometer brand Kistler, model 9257 BA, acquisition in 3 working ranges in F_x , F_y and F_z from 0.5 kN to 10 kN, acquisition rate of 2 kHz (F_x , F_y) and 3.5 kHz (F_z) and a 3-channel charge amplifier, Kistler, model 5233A. A National Instruments AD data acquisition board, model NI-USB-6221 was used for the conversion and transmission of analog to digital signals. Figure 3 represents the assembly of samples for acquisition of machining force data, during the milling process.

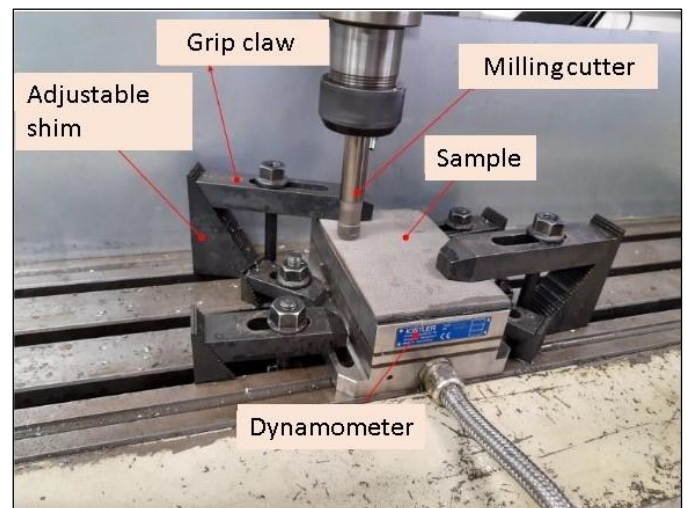


Figure 3: Assembly of samples.

Source: Authors, (2022).

For the acquisition of roughness data, a Mitutoyo rugosimeter, model SJ-210, was used, with a probe of 5 $\mu\text{m/s}$, cut off 0.8 mm and resolution of 0.01 μm . In each milled slot, 3 measurements were taken.

The preparation of the machined surface for evaluation of the surface finish was carried out by two passes with a depth of 0.5 mm in each groove. The experimental values measured were considered after the execution of the 2nd pass (denoted new tool) and 6th pass (denoted worn tool) of machining. In the evaluation of the surface finish attributed to the samples, the parameters R_a (with corresponding mean values and standard deviation), R_z and R_t (with their maximum values) were considered.

It is important to highlight that, in the samples with and without sealant machined with a cutting speed of 84 m/min, there was a strong vibration in the process, which was more intense in the sample with sealant.

IV. RESULTS AND DISCUSSIONS

IV.1 WITH VARIATION OF CUTTING SPEED

In the evaluation of the coating, considering the variation of cutting speed with 50 m/min and 84 m/min, it was observed how these speeds influenced the machining force, the surface finish and tool wear. The best results were obtained with a cutting speed of 50 m/min based on machining forces and tool wear analysis, although the presence of the sealant did not impact the surface quality, given the variation in cutting speed.

It can be highlighted, in the machining of samples with and without sealant with a speed of 84 m/min, the presence of strong vibration in the process. Though vibration has been more intense in the sample with sealant. This fact resulted in expressive tool wear, as well as an increase in the machining force.

IV.2 WITH CONSTANT CUTTING SPEED

Cutting speed was set to 50m/min because it demonstrated better performance in terms of machining forces and tool wear. Having defined the best cutting parameters, the following tests were carried out with tools with radius of 0.4 mm and 0.8 mm, using a cutting speed of 50 m/min.

IV.2.1 CUTTING TOOL WEAR

Nose flank wear is notably evident on the main flank, as shown in Figures 4 and 5.

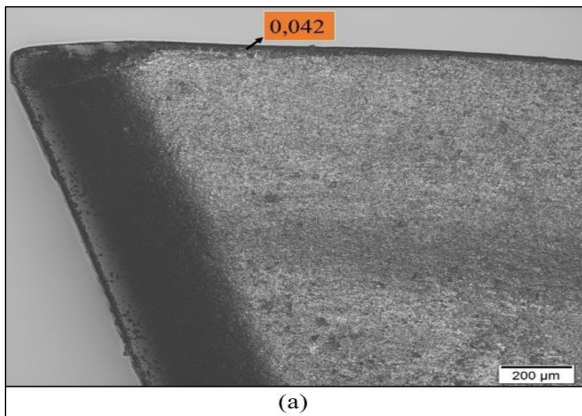


Figure 4a: Wear on the main flank with insert 0,4 mm: (a) Without sealant.
Source: Authors, (2022).

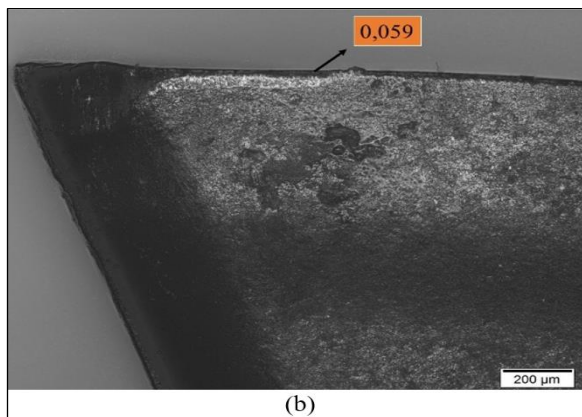


Figure 4b: Wear on the main flank with insert 0,4 mm: (b) With sealant.
Source: Authors, (2022).

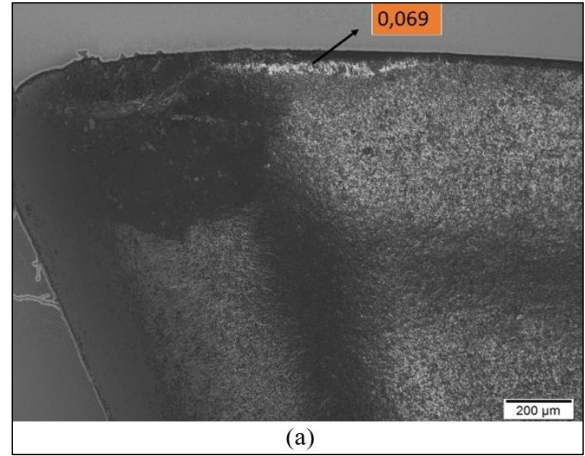


Figure 5a: Wear on the main flank with insert 0,8 mm: (a) Without sealant.
Source: Authors, (2022).

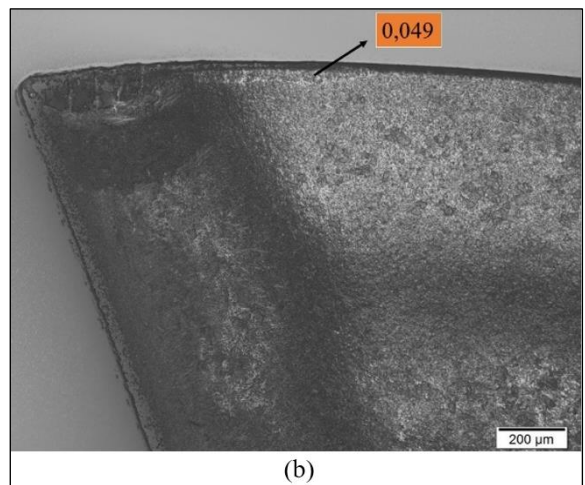


Figure 5b: Wear on the main flank with insert 0,8 mm: (b) With sealant.
Source: Authors, (2022).

Figures 6 and 7 show the predominant wear characteristic located at the tool tip, in the secondary flank region. The phenomenon of adhesion is present, mainly on the flank of the tool with a radius of 0.4mm, when milling the material without sealant, illustrated in Figure 6a.

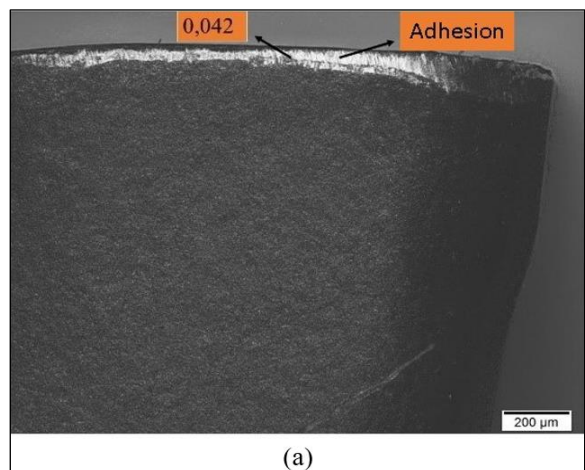


Figure 6a: Wear on the secondary flank with insert 0,4 mm: (a) Without sealant.
Source: Authors, (2022).

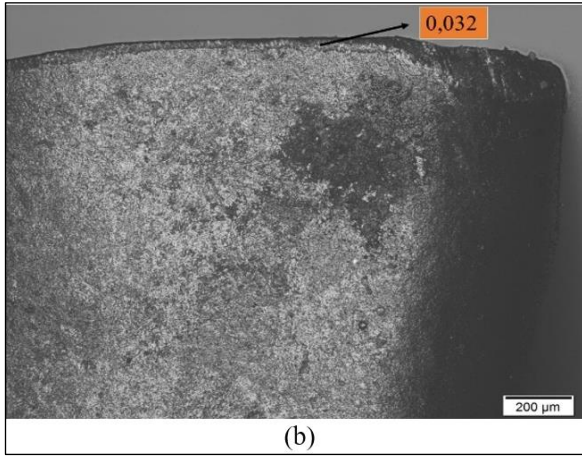


Figure 6b: Wear on the secondary flank with insert 0,4 mm: (b) With sealant.
Source: Authors, (2022).

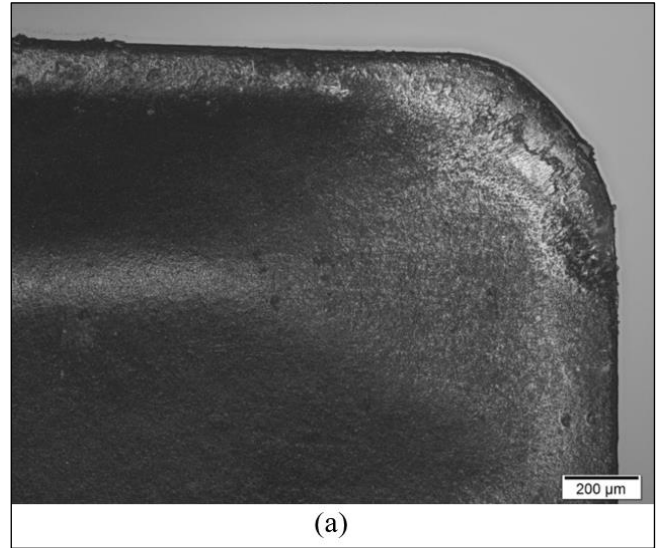


Figure 8a: Wear on the cutting tool rake face with insert 0,4 mm: (a) Without sealant.
Source: Authors, (2022).

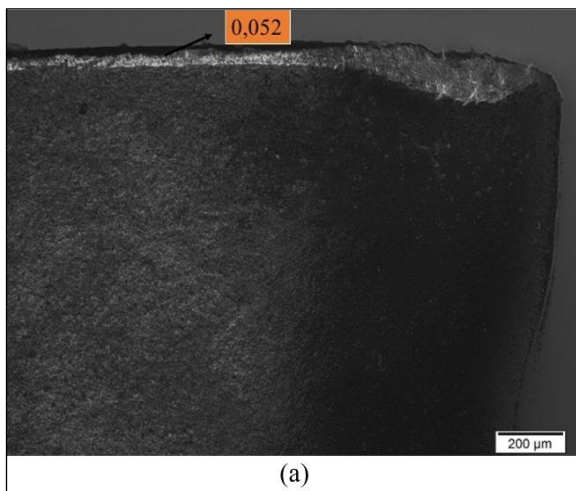


Figure 7a: Wear on the secondary flank with insert 0,8 mm: (a) Without sealant.
Source: Authors, (2022).

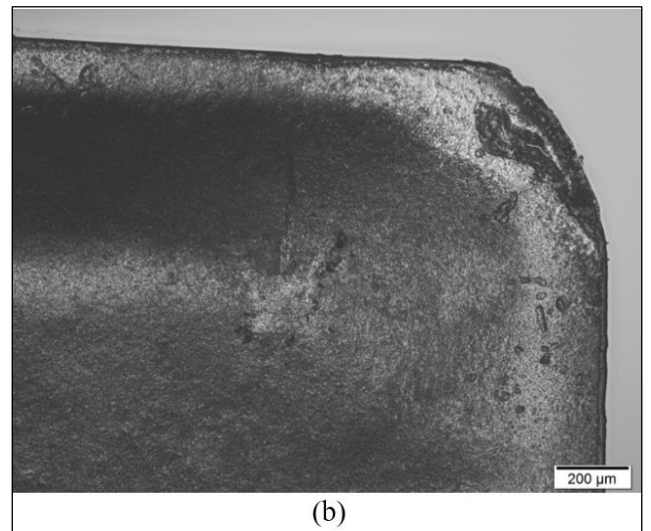


Figure 8b: Wear on the cutting tool rake face with insert 0,4 mm: (b) With sealant.
Source: Authors, (2022).

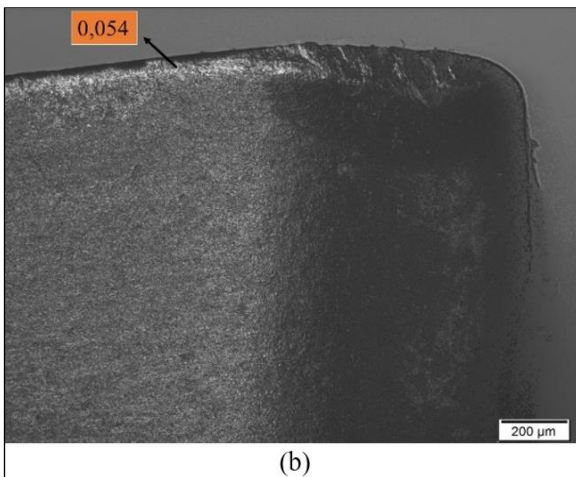


Figure 7b: Wear on the secondary flank with insert 0,8 mm: (b) With sealant.
Source: Authors, (2022).

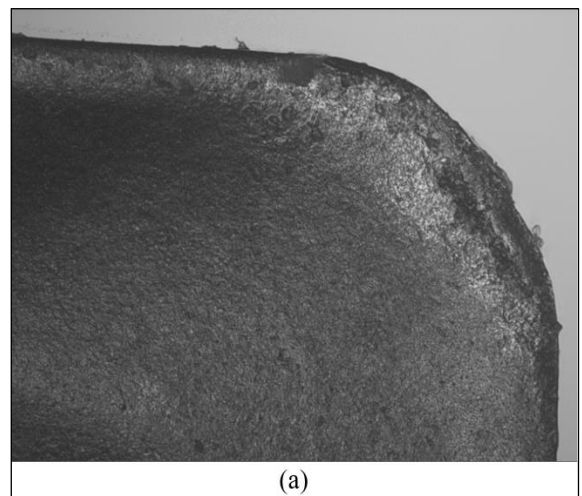


Figure 9a: Wear on the cutting tool rake surface with insert 0,8 mm: (a) Without sealant.
Source: Authors, (2022).

Crater wear caused by plastic deformation on the rake face can be seen in Figures 8 and 9. The wear is more pronounced on inserts with a 0.8mm radius, as seen in Figures 9a and 9b.

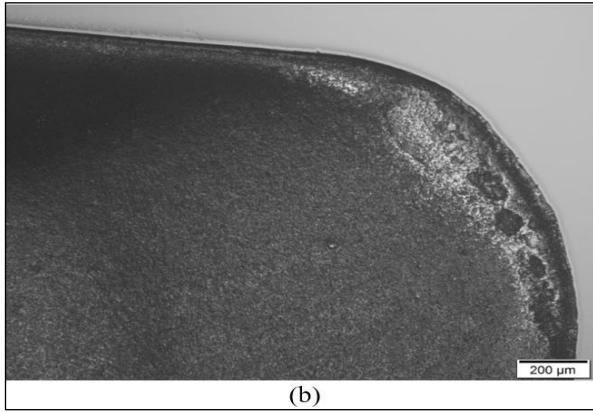


Figure 9b: Wear on the cutting tool rake surface with insert 0,8 mm: (b) With sealant. Source: Authors, (2022).

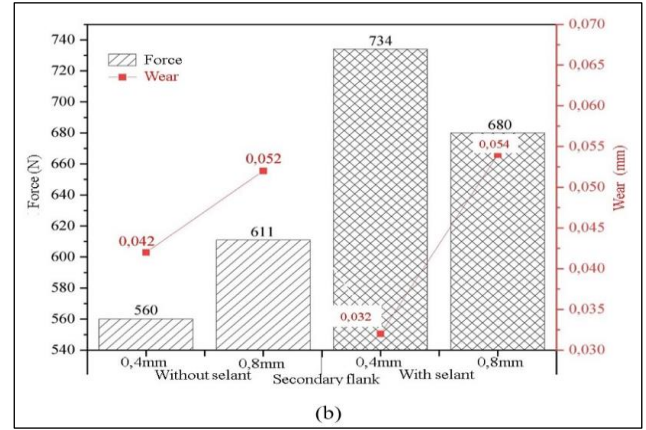


Figure 10b: Machining forces x wear: (b) Secondary flank. Source: Authors, (2022).

IV.2.2 Machining Force and Wear on Cutting Tools

Figures 10a and 10b represent the values corresponding to the machining forces and wear on the inserts, at the end of the milling process, where the inserts are in the worn condition. Analyzing the machining forces acting, it is noted the predominance of the highest values in the samples with sealant. The effect of machining in these samples can be attributed to the typical behavior of the cutting mechanism in fiber-reinforced composites, where hard polymer particles are formed during tool sliding. Studying the effect of milling carbon fiber-reinforced polymer composites, [17] admitted the possibility of the milling process inducing delamination during machining. The shear forces act by pushing the unsupported fibers, resulting in delamination of the composite material. The presence of protruding fibers on the machined surface prevents the tool edge from passing through, thus increasing the friction force.

With reference to the insert with 0.4mm radius, there was less machining force with less wear, when milling the samples without sealant. However, with the application of the sealant, the machining force and wear were higher (mainly on the main flank) compared to the insert with a radius of 0.8 mm, as shown in Figures 10a and 10b. [18] performed a check on the behavior of the cutting force through the ratio r/h (insert tip radius / depth of cut) greater and less than unity. Uncoated carbide inserts were used for milling glass fiber reinforced polymer (GFRP) sheets. The r/h parameter was investigated for different tool nose radius. The researchers found that there was a disproportionate increase in shear forces in the $r/h < 1$ condition, a fact repeated in this work, as reported above.

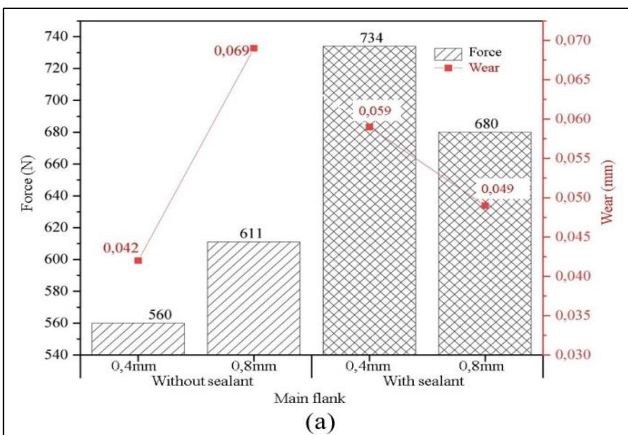


Figure 10a: Machining forces x wear: (a) Main flank. Source: Authors, (2022).

IV.2.3 Machining Force and Surface Finish

As can be seen in figures 11a and 11b, there was a tendency towards higher average roughness values in the samples coated with sealant. However, there are no significant differences in the values presented. The experimental values obtained remained satisfactory, according to the limits proposed in the literature. It is also noted that the tool with a radius of 0.4 mm on the sample without sealant produced a better final finish, with less machining effort.

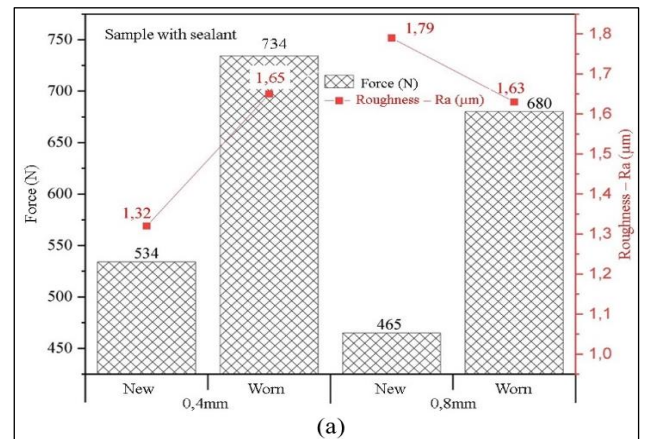


Figure 11a: Machining force x surface finish: (a) Samples with sealant. Source: Authors, (2022).

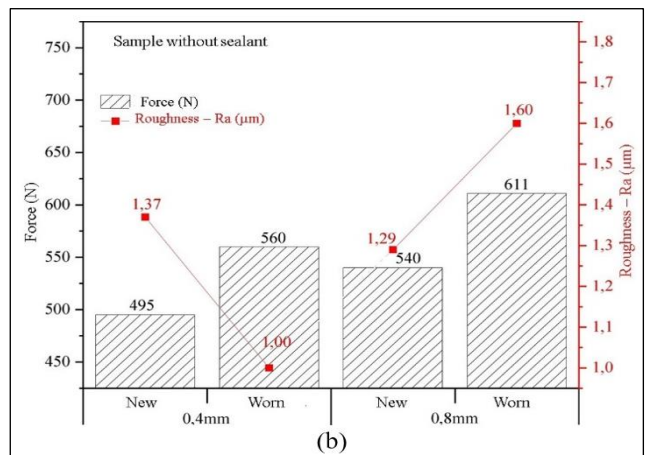


Figure 11b: Machining force x surface finish: (b) Samples without sealant. Source: Authors, (2022).

IV.3 ANALYSIS OF MACHINED SURFACES

With reference to the surfaces of the sample without sealant machined with inserts with a radius of 0.8 mm (Figure 12a), visible tool marks are noted on the machined surface in the 3rd groove. This fact is probably due to the wear on the flanks and the plastic deformation that occurred at the tips of the inserts, as can be seen in Figures 14a and 16a. The highest value of machining force used is observed with the insert with a radius of 0.8 mm, in comparison with the insert with a radius of 0.4 mm, as shown in Figure 10a. According to [19], plastic deformation originates from the action of cutting forces and stresses on the cutting edge at high temperatures, which reduces the mechanical properties of the tool, making it vulnerable to wear. The spectrum of the machining force at the end of the milling process can be seen in Figure 12b.

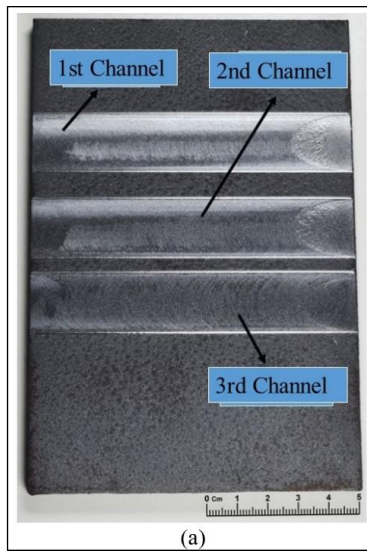


Figure 12a: Sample without sealant (nose radius 0,8 mm): (a) Machined surfaces.
Source: Authors, (2022).

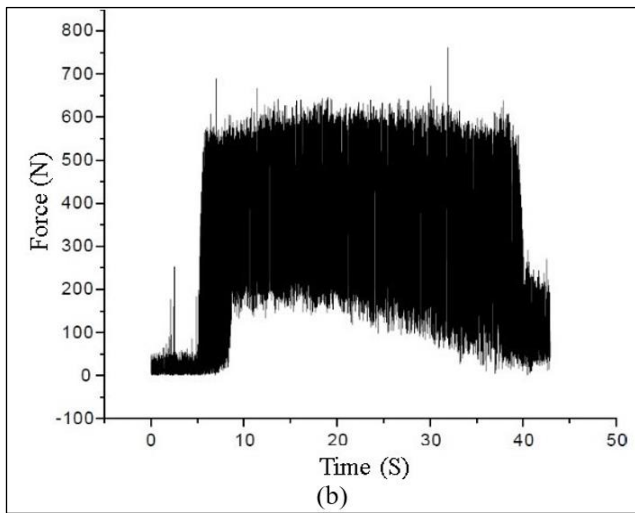


Figure 12b: Sample without sealant (nose radius 0,8 mm): (b) Force spectrum (3rd channel).
Source: Authors, (2022).

In the case of the sample with sealant milled with a radius of 0.8 mm (Figure 13a), the machined channels also have tool marks on their surfaces due to the same reason attributed to the samples without sealant, previously described. Less wear is

observed on the main flank, in relation to the sample with sealant machined with a radius of 0.4 mm, as shown in Figure 10a. The behavior of the machining forces acting on the cutting edge can be described in the spectrum indicated in Figure 13b.



Figure 13a: Sample with sealant (nose radius 0,8 mm): (a) Machined surfaces.
Source: Authors, (2022).

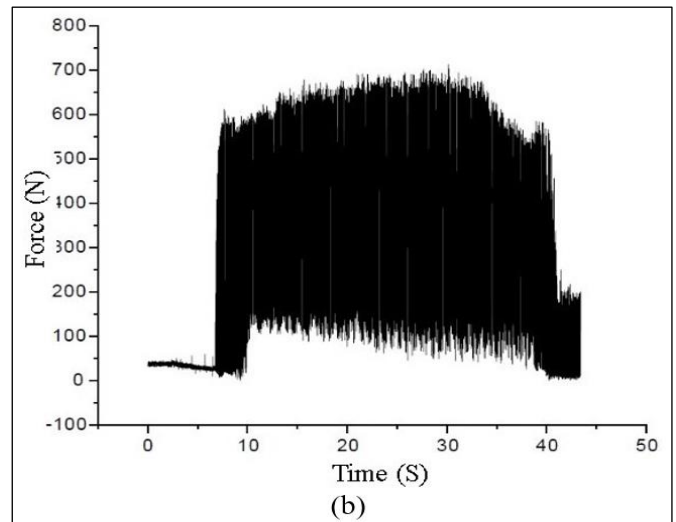


Figure 13b: Sample with sealant (nose radius 0,8 mm): (b) Force spectrum (3rd channel).
Source: Authors, (2022).

When milling the sample with a sealant machined with an insert with a radius of 0.4 mm expressed in Figure 14a, the deep marks of the cutting tool on the machined surface can be seen in the 2nd groove, which must have increased the wear on the flanks and on the tip of the wafer, as shown in Figures 4b and 6b. According to [20], grooves on the machined surface are attributed to the bearing of hard particles between the tool-workpiece interface. These particles penetrate the grooves and cavities of the worn surface of the tool, acting on the machined surface. This fact resulted in an increase in the machining force and greater wear on the main flank, compared to the wear and machining force acting on the 0.8mm radius insert, as shown in Figure 10a. At the end of the milling process, the machining forces were maintained according to the spectrum in Figure 14b.



Figure 14a: Sample with sealant (nose radius 0,4 mm): (a) Machined surfaces.
Source: Authors, (2022).

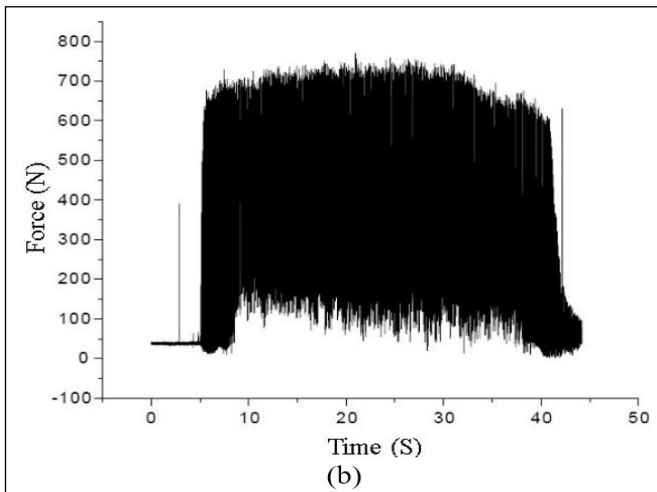


Figure 14b: Sample with sealant (nose radius 0,4 mm): (b) Force spectrum (3rd channel).
Source: Authors, (2022).

Observing Figure 15a, which depicts the milling on the sample without sealant machined with an insert with a radius of 0.4 mm, one can see, in the machining of the 3rd groove, a surface finish with gloss, tool marks and a roughness value below the found, as discussed in Figure 11b. What may have occurred in the machining of this groove, due to the loss of coating, was the adhesion of the material to the edge of the cutting insert, as shown in Figure 6a. There was no shear in the action of the cutting edge on the material, but the plasticization of the coating sprayed on the machined surface. This phenomenon is called melting. According to [21], the melting is related to the adhesion of the sample material on the cutting edge of the tool, causing an increase in temperature at the interface of the tool and the surface of the sample, due to friction. Consequently, there is a reduction in the mechanical strength and plasticity of the sample material. However, [22] indicate that, to the coating of carbide tools, the characteristic of increasing the adhesion resistance is attributed, facilitating the flow and removal of the chip.

The force spectrum shown in Figure 15b, indicates the presence of melting on the surface of the sample without sealant

machined with a tool with a radius of 0.4 mm, at the end of the milling process.

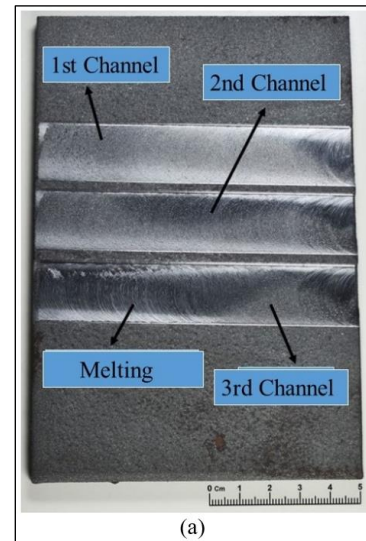


Figure 15a: Sample without sealant (nose radius 0,4 mm): (a) Machined surfaces.
Source: Authors, (2022).

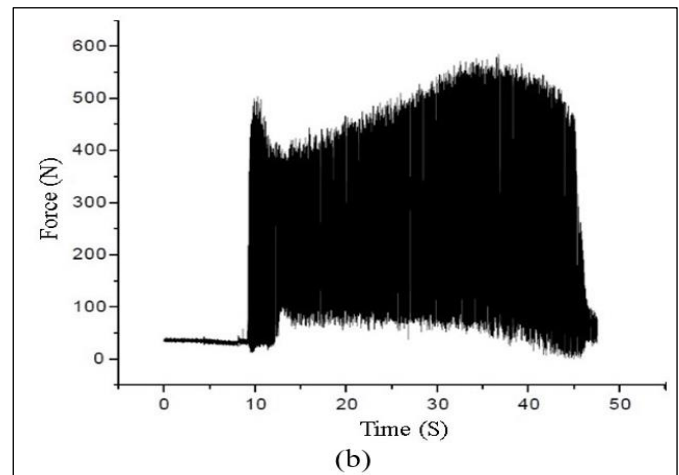


Figure 15b: Sample without sealant (nose radius 0,4 mm): (b) Force spectrum (3rd channel).
Source: Authors, (2022).

V. CONCLUSIONS

Due to the results obtained, it is possible to conclude that:

1. The current thermal sprayed demonstrated high surface roughness and high porosity, which are intrinsic from the arc spray process, resulting intermittent cutting;
2. The presence of sealant on the coating provided an increase in the machining force. Due to the sealant being an epoxy resin, the typical behavior of the cutting mechanism may have occurred in composite materials in which hard polymer particles are formed during milling, increasing the machining force;
3. In the machining process of the coating with the highest cutting speed (84 m/min), and with an insert with a radius of 0.8 mm, there was strong vibration, and the highest values of machining force were recorded, especially in the sample with sealant application;

4. The wear on the tip, which occurred as a result of the friction between the insert tip and the part, and the crater wear, as a result of the friction between the tool and the chip, were the most expressive in cutting tools;
5. The quality of the machined surface did not show relevant differences, where the average roughness remained within the standard of the literature in tools with or without sealant;
6. In machining with cutting speed of 50 m/min and spray coating without application of sealant, the insert with 0.4 mm radius showed more favorable results such as lower machining force, less wear and better finish on the machined surface;
7. The 0.8 mm radius insert showed better performance when machining the specimen with sealant with lower machining force, less tool wear on the main flank and slightly lower surface roughness.

VI. AUTHOR'S CONTRIBUTION

Conceptualization: Carlos Jorge Leão de Oliveira, Hector Reynaldo Meneses Costa, Tatiane de Campos Chuvas and Rafael da Cunha Hamano.

Methodology: Carlos Jorge Leão de Oliveira and Tatiane de Campos Chuvas.

Investigation: Carlos Jorge Leão de Oliveira and Rafael da Cunha Hamano.

Discussion of results: Carlos Jorge Leão de Oliveira and Tatiane de Campos Chuvas.

Writing – Original Draft: Carlos Jorge Leão de Oliveira.

Writing – Review and Editing: Carlos Jorge Leão de Oliveira, Rafael da Cunha Hamano and Tatiane de Campos Chuvas.

Resources: Carlos Jorge Leão de Oliveira and Hector Reynaldo Meneses Costa.

Supervision: Hector Reynaldo Meneses Costa and Tatiane de Campos Chuvas.

Approval of the final text: Carlos Jorge Leão de Oliveira, Hector Reynaldo Meneses Costa, Tatiane de Campos Chuvas and Rafael da Cunha Hamano.

VII. ACKNOWLEDGMENTS

The authors would like to thank the following institutions for the support given during the execution of the present work: CEFET-RJ, CTEEx, CNPq, CAPES and FAPERJ.

VIII. REFERENCES

- [1] R. Varavallo, M. D. Manfrinato, L. S. Rossino, F. Camargo, e S. D. de Souza, "Ensaio de adesão em revestimentos metálicos obtidos por HVOF", p. 1–6, jul. 2008.
- [2] J. Řehoř et al., "Prediction Of The Influence Of Cutting Conditions On Surface Morphology After Its Thermal Spraying With Stellite 6 Alloy", In Review, preprint, fev. 2022. doi: 10.21203/rs.3.rs-1336218/v1.
- [3] T. Zlámal, J. Petrů, M. Pagáč, e P. Krajčovič, "Influence of Machining Process on Surface Integrity of Plasma Coating", vol. 11, no 12, p. 5, 2017.
- [4] M. Gueli, J. Ma, N. Cococetta, D. Pearl, e M. P. Jahan, "Experimental investigation into tool wear, cutting forces, and resulting surface finish during dry and flood coolant slot milling of Inconel 718", *Procedia Manuf.*, vol. 53, p. 236–245, 2021, doi: 10.1016/j.promfg.2021.06.026.
- [5] P. Das, S. Paul, e P. P. Bandyopadhyay, "Plasma sprayed diamond reinforced molybdenum coatings", *J. Alloys Compd.*, vol. 767, p. 448–455, 2018, doi: 10.1016/j.jallcom.2018.07.088.
- [6] J.-K. Xiao, Y.-Q. Wu, W. Zhang, J. Chen, X.-L. Wei, e C. Zhang, "Microstructure, wear and corrosion behaviors of plasma sprayed NiCrBSi-Zr coating", *Surf. Coat. Technol.*, vol. 360, p. 172–180, fev. 2019, doi: 10.1016/j.surfcoat.2018.12.114.
- [7] G. Darut et al., "State of the art of particle emissions in thermal spraying and other high energy processes based on metal powders", *J. Clean. Prod.*, vol. 303, p. 126952, jun. 2021, doi: 10.1016/j.jclepro.2021.126952.
- [8] W. Chen et al., "Friction and anti-corrosion characteristics of arc sprayed Al+Zn coatings on steel structures prepared in atmospheric environment", *J. Mater. Res. Technol.*, vol. 15, p. 6562–6573, nov. 2021, doi: 10.1016/j.jmrt.2021.11.084.
- [9] M. M. Verdian, "3.13 Finishing and Post-Treatment of Thermal Spray Coatings", em *Comprehensive Materials Finishing*, Elsevier, 2017, p. 191–206. doi: 10.1016/B978-0-12-803581-8.09200-6.
- [10] M. Vijaya Ganesa Velan, M. Subha Shree, e P. Muthuswamy, "Effect of cutting parameters and high-pressure coolant on forces, surface roughness and tool life in turning AISI 1045 steel", *Mater. Today Proc.*, vol. 43, p. 482–489, 2021, doi: 10.1016/j.matpr.2020.12.020.
- [11] Araújo, Anna Carla (último), Mougo, Adriane Lopes, e Campos, Fábio de Oliveira. *Usinagem para Engenharia - Um Curso de Mecânica do Corte*, 1a. Rio de Janeiro - BR, 2020.
- [12] Y. Chen, J. Wang, e Q. An, "Mechanisms and predictive force models for machining with rake face textured cutting tools under orthogonal cutting conditions", *Int. J. Mech. Sci.*, vol. 195, p. 106246, abr. 2021, doi: 10.1016/j.ijmecsci.2020.106246.
- [13] G. Jangali Satish, V. N. Gaitonde, e V. N. Kulkarni, "Traditional and non-traditional machining of nickel-based superalloys: A brief review", *Mater. Today Proc.*, vol. 44, p. 1448–1454, 2021, doi: 10.1016/j.matpr.2020.11.632.
- [14] Z. Barzegar e E. Ozlu, "Analytical prediction of cutting tool temperature distribution in orthogonal cutting including third deformation zone", *J. Manuf. Process.*, vol. 67, p. 325–344, jul. 2021, doi: 10.1016/j.jmapro.2021.05.003.
- [15] ASTM, "ASTM A36: Standard Specification for Carbon Structural Steel", p. 6, 1977.
- [16] Norma ASME, "ASME SECTION II - Materials - ASME Boiler and Pressure Vessel code an International code", no 2021, p. 1019, 2021.
- [17] F. Romeo Martins, "Caracterização do fresamento de chapas de compósito polímero reforçado com fibras de carbono (PRFC)", *Doutor em Engenharia Mecânica*, Universidade Estadual de Campinas, Campinas, 2014. doi: 10.47749/T/UNICAMP.2014.931949.
- [18] V. Schulze, C. Becke, e R. Pabst, "Specific machining forces and resultant force vectors for machining of reinforced plastics", *CIRP Ann.*, vol. 60, no 1, p. 69–72, 2011, doi: 10.1016/j.cirp.2011.03.085.
- [19] W. Akhtar, J. Sun, P. Sun, W. Chen, e Z. Saleem, "Tool wear mechanisms in the machining of Nickel based super-alloys: A review", *Front. Mech. Eng.*, vol. 9, no 2, p. 106–119, jun. 2014, doi: 10.1007/s11465-014-0301-2.
- [20] M. Sarikaya et al., "A state-of-the-art review on tool wear and surface integrity characteristics in machining of superalloys", *CIRP J. Manuf. Sci. Technol.*, vol. 35, p. 624–658, nov. 2021, doi: 10.1016/j.cirpj.2021.08.005.
- [21] J. M. Zhou, V. Bushlya, e J. E. Stahl, "An investigation of surface damage in the high speed turning of Inconel 718 with use of whisker reinforced ceramic tools", *J. Mater. Process. Technol.*, vol. 212, no 2, p. 372–384, fev. 2012, doi: 10.1016/j.jmatprotec.2011.09.022.
- [22] B. C. M. Reis et al., "Influência do material da ferramenta de corte sobre a usinabilidade do aço ABNT 4340 no torneamento", *Matér. Rio Jan.*, vol. 24, no 3, p. e12449, 2019, doi: 10.1590/s1517-707620190003.0765.